Published in final edited form as:
Exp Cell Res. 2015 January 1; 330(1): 222–232. doi:10.1016/j.yexcr.2014.08.020.

Interactive relationship between basement-membrane development and sarcomerogenesis in single cardiomyocytes

Huaxiao Yang[1], **Thomas K. Borg**[2], **Honghai Liu**[3], and **Bruce Z. Gao**[1]

[1]Department of Bioengineering, Clemson University, SC, United States

[2]Department of Regenerative Medicine, Medical University of South Carolina, SC, United States

[3]Department of Pathology, University of Cincinnati, OH, United States

Abstract

The cardiac basement membrane (BM), the highly organized layer of the extracellular matrix (ECM) on the external side of the sarcolemma, is mainly composed of laminin and collagen IV, which assemble a dense, well-organized network to surround the surface of each adult cardiomyocyte. The development of the cardiac BM plays a key role in organogenesis of the myocardium through interactions between sarcomeres and integrins. Because of the complicated structure of cardiac muscle fibers and lack of a proper investigation method, the detailed interactions among BM development, sarcomeric growth, and integrin expression remain unclear. In this study, freshly isolated 3-day neonatal cardiomyocytes (CMs) were cultured on aligned collagen, which mimics the in vivo ECM structure and induces neonatal CMs to grow into rod-like shapes. Then double fluorescence-immunostained laminin and α-actinin or integrin β1 on neonatal CMs cultured 4-72 h were imaged using a confocal microscope, and the spatial relationship between laminin deposition and α-actinin expression was evaluated by colocalization analysis. At 4 h, laminin was deposited around Z-bodies (dot-shaped α-actinin) and integrins; from 18-to-72 h, its gradual colocalization with Z-lines (line-shaped α-actinin) and integrins increased Pearson's coefficient; this indicates that development of the BM network from the neonatal stage to adulthood is closely related to sarcomeric formation via integrin-mediated interactions.

Keywords

basement membrane; laminin; sarcomerogenesis; Z-lines; integrin

Author to whom correspondence should be addressed, zgao@clemson.edu; Tel.: +1-864-656-0185; Fax: +1-864-656-4466.

Introduction

The basement membrane (BM), the highly organized layer of the extracellular matrix (ECM) on the external side of the sarcolemma, is composed of numerous glycoproteins and proteoglycans, such as type IV collagens, laminins, entactins, perlecan, and chondroitin sulfate proteoglycans (6, 35). The BM is structurally or functionally associated with various cell types, such as endothelial cells, podocytes (19), aortic smooth muscle cells (29), tracheal epithelial cells (8), Schwann cells (17), and cardiomyocytes (CMs) (15); it first appears during the blastocyst stage between the primitive endoderm and the inner cell mass and is the first ECM produced during embryogenesis (13). In different organs and tissues, the BM network takes different paths of development and maturation. For example, during glomerulogenesis in the kidney, laminin $\alpha1\beta1\gamma1$ and $\alpha4\beta1\gamma1$ are both present from the comma-shape through the S-shape stages. They are rapidly removed during the capillary-loop stage, and laminin $\alpha5\beta2\gamma1$ is deposited in the glomerular BM (GBM) throughout adulthood (1). In the human heart, several subunits of laminin have been detected; for example, at Gestational Week 8, laminin $\beta1$ and $\beta2$ were found in the ECM that surrounds CMs and in the BM zone of the endo/pericardium (22). After birth, collagen IV is increasingly deposited in the endomysium from Day 0-Day 3, and collagen fibers form a densely woven network that surrounds groups of CMs (3). Observation of adult CMs with transmission electron microscopy shows that the BM forms a dense network around each adult CM (12). During dedifferentiation and redifferentiation of adult CMs cultured in vitro, the BM forms a fine network radiating from the central area near the nucleus to the pseudopods (15).

The BM's unique structural relationship with its associated tissues makes it critical in organogenesis of a variety of organs and tissues. For example, GBM is instrumental in glomerulogenesis; without GBM, a glomerular cell is unable to maintain its position, leading to a disorganized glomerulus (18). In the circulatory system, blood-vessel maturation requires the presence of laminin $\alpha4\beta1\gamma1$ (8). In skeletal muscle, the BM contributes to differentiation of the myotube and is crucial in development of the neuromuscular junction (20). In heart muscle, the BM network is influential in sarcomeric formation and remodeling because of its interaction with integrins, which serve as receptors on the plasma membrane and orchestrate multiple myocardial functions, including organogenesis (24). For example, integrins $\alpha1\beta1$ and $\alpha3\beta1$ can directly bind with laminin to sense outside-in signals (24) and transfer them to the sarcomeres near the Z-line (4). Although the BM-integrin-sarcomere complex is known to mediate growth and differentiation of neonatal cardiomyocytes (CMs) (23), BM involvement in sarcomerogenesis has not been studied. Particularly, fundamental knowledge of the spatial correlation between distribution of the BM network and the Z-lines during development of a single neonatal CM is poorly understood. The network formation around a single CM during its development from a neonate to an adult is largely unknown because of the complicated structure of cardiac-muscle fibers and lack of a comprehensive in vitro culture model.

A substrate coated with an aligned collagen using the method used by Ross and coworkers (27) was found to promote in vitro neonatal CMs to form in vivo-like cardiac muscle-fiber structures. This type of substrate was utilized to study sarcomerogenesis of cardiac cells (26)

and was demonstrated to maintain neonatal CMs in the rod-like phenotype that is typical of Week 4.

In this study, confocal images of single neonatal CMs cultured from 4-72 h on aligned collagen were analyzed sequentially. The purpose of this study was to examine the sequential formation of the sarcomere in relation to expression of basement membrane (laminin), α-actinin, and integrin β1. According to our unpublished data, BM-collagen IV, another major component of the BM, shows a different pattern of formation around the neonatal CMs in comparison to BM-laminin; its expression may be closely related to cardiomyocyte-fibroblast interactions. The study of CM BM-collagen IV will be reported in our future publications.

Methods and Materials

Cell harvest and culture

Adult Sprague–Dawley (SD) rats and 3-day-old neonatal SD rats were euthanized according to a procedure approved by the Clemson University Institutional Animal Care and Use Committee (Protocol number AUP2013-035). The procedure conforms to the Guide for the Care and Use of Laboratory Animals published by the US National Institutes of Health (NIH Publication, 8th Edition, 2011). The methods of euthanasia for neonatal and adult animals are consistent with the recommendations of the Panel on Euthanasia of the American Veterinary Medical Association.

Neonatal CM harvest—Neonatal CMs were isolated from 3-day-old SD rats using the two-day protocol we previously reported (16). In brief, ten neonatal rats were dissected, and the hearts were collected and minced in Moscona's saline. The tissue was transferred to 50 ml Dulbecco's Phosphate Buffered Saline (DPBS) with 4 mg trypsin and 50 mg neutral protease and stored in a 4° C refrigerator overnight. The next day, the tissue was transferred into 50 ml Kreb's Ringers Bicarbonate Buffer (KRB) with 10 mg collagenase type I and 30 mg collagenase type II and then shaken in a water bath at 50 rpm for 45-60 min. The cell suspension was washed twice using cardiomyocyte culture medium (high glucose Dulbecco's Modified Eagle's Medium (DMEM) supplemented with 10% fetal bovine serum and 1% penicillin streptomycin) to remove enzyme residue. The isolated cells were transferred into a 150 cm^2 flask for a cell-adhesive assay to remove cardiac fibroblasts. After two hours, the unattached neonatal CMs were collected for use. Our immunofluorescence staining data and data from other groups that used the same neonatal CM purification procedure have demonstrated that 95% neonatal CM purification can be achieved.

Adult CM harvest—Adult CMs were harvested from the hearts of one-month-old adult SD rats (33). In brief, after a heparin injection (45 mg/kg) and the intraperitoneal sodium pentobarbital injection (0.5 ml/100g) that followed, the heart with at least 5 mm of the aortic arch was removed and placed in the perfusion buffer. The heart was then perfused through the aortic arch with the perfusion buffer for 5 minutes at a flow rate of 12 ml/min. The perfusion buffer was replaced with a digestive buffer, and the heart was perfused for 60 minutes at a flow rate of 6 ml/min. Once enzymatic digestion of the heart was complete, the ventricle was placed in a 100 mm dish containing 5 ml of digestion buffer and gently

minced into small pieces (~ 1 mm^3) with fine forceps. The cell suspension was transferred to a 50 ml conical polypropylene tube. Approximately 5 ml of perfusion buffer (37 °C) was added to the tube to create a final cell-suspension volume of 40 ml. After agitation, a stop buffer (10 ml) was added and mixed well using a 50 ml plastic transfer pipette; this was followed by ten gentle agitations of the solution with the pipette. The cell clumps were then allowed to settle by gravity sedimentation for 2 minutes, and the supernatant was transferred into a new 50 ml tube. Another 40 ml perfusion buffer was added to the original tube, and the above procedures were repeated until very few pieces of tissue were left in the tube. The collected supernatant was centrifuged for 3 minutes at 500 rpm. The supernatant was carefully removed from the centrifuged tube. The pellet was resuspended in a 50 ml tube with 20 ml perfusion buffer and agitated gently 10 times. The resuspended cells then underwent calcium reintroduction followed by centrifugation for 3 minutes at 500 rpm. The supernatant was removed, and the resuspended cells in culture medium (5000 cells/ml) were ready for use.

In vitro culture of neonatal CMs—The freshly isolated neonatal CMs were cultured on aligned collagen I gel. The aligned collagen-coated coverslip was fabricated as follows: Type I collagen gel was prepared by mixing rat type I collagen solution (3.1 mg/mL, Advanced Biomatrix, Ltd., US) with HEPES solution (0.1M, pH = 9.0) at a ratio of 3:7 on an ice bath without intensive pipetting. A drop of pre-gel solution (~500 μL) was added to the surface of a clean 22×22 mm glass coverslip. After 30 s, the pre-gel had covered the glass surface; the solution was sucked off, leaving a very thin layer of collagen pre-gel on the glass. Then the coverslip was placed for at least 1 h into an incubator (37 °C and 5% CO_2) inclined at 30° to form aligned collagen fibers. After incubation, the surface of the coverslip was rinsed with a PBS buffer; 1 ml freshly isolated neonatal CMs ($5x10^5$/ml) was seeded onto the aligned collagen-coated coverslip, which was then cultured in an incubator (37 °C and 5% CO_2).

Tissue preparation and sectioning

The ventricles from 4-month-old adult SD rats were used to prepare ventricular-tissue slides with microtome-cyrostat sectioning. After being fixed in 4% paraformaldehyde for 24 h at 4 °C and washed with PBS three times, all tissues were frozen at -20 °C in tissue-freezing medium (Tissue-Tek OCT compound, Sakura Finetechnical Co., Ltd, Japan). Immediately after freezing, the tissues were cut into 20 μm sections using a cryostat (Leica CM1950, Wetzlar, Germany) to produce transverse-tissue slides (perpendicular to the interventricular septum).

The procedures of immunofluorescence staining

Laminin staining of adult CMs, neonatal CMs, and ventricular-tissue sections

Adult CMs: Freshly isolated adult CMs were suspended and fixed in a 4% paraformaldehyde (pH 7.4) solution for 15 minutes at room temperature (RT) and then centrifuged at 500 rpm for 3 minutes, suspended with blocking solution (4% (v/v) goat serum and 1% (v/v) BSA in PBS solution) for 30 minutes at RT, then centrifuged at 500 rpm for 3 minutes and suspended in 2 ml rabbit-anti-rat laminin PBS solution (1:300, LAMA 1,

Abcam Inc., US) overnight at 4 °C. They were then centrifuged at 500 rpm for 3 minutes and washed 3 times with PBS and suspended with 2 ml FITC conjugated IgG goat-anti-rabbit PBS solution (1:200, Life Technologies, US) for 1.5 h at RT. The cells were washed with PBS three times, and finally they were suspended with ProLong© Antifade Kit mounting medium (Life Technologies, US). A drop of the resultant cell solution (20 μL) was placed on a glass slide and covered with a coverslip.

Neonatal CMs: First, neonatal CMs cultured on aligned collagen-coated coverslips for 1, 4, 20, 24, 48, and 72 h were fixed in 4% paraformaldehyde (pH 7.4) solution for 15 minutes at RT and then treated using steps similar to those for immunofluorescence staining of adult CMs. Coverslips were mounted with ProLong© Antifade Kit mounting medium (Life Technologies, US) for fluorescent imaging later.

Ventricular tissue sections: The frozen tissue sections stored in -20 °C were brought to RT for a period of 30 min and then incubated with 0.025% Triton X-100 (Sigma, US) for 30 min at RT. The remaining steps were the same as those for staining neonatal CMs.

Double staining of neonatal CM laminin and α-actinin: After each step of incubation with antibodies, samples were washed with PBS three times for 10 min each time. Neonatal CMs cultured on aligned collagen-coated coverslips were fixed at culture stages of 4, 18, 48, and 72 h. The fixed sample was first stained for α-actinin: It was blocked with 1% BSA, 4% donkey serum, 0.025% Triton X-100, and PBS for 30 minutes at RT. Next, the sample was incubated with the first antibody, mouse-anti-rat α-actinin (1:500, Sigma, US), overnight at 4 °C. It was then incubated with the second antibody, Alexa fluor © 488 conjugated donkey-anti-mouse IgG (1:200, Life Technologies, US), for 1.5 h in the dark at RT. The sample was stained for laminin and blocked again with 1% BSA, 4% goat serum and PBS for 30 minutes at RT. It was incubated with the first antibody, rabbit-anti-rat laminin (1:200, Abcam, US) overnight at 4 °C. It was then incubated with the second antibody, Alexa fluor© 594 coagulated goat-anti-rabbit IgG (1:200, Life Technologies, US), for 1.5 h at RT in the dark. After being mounted with ProLong© Antifade Kit medium (Life Technologies, US), the sample was ready for observation.

Double staining of laminin and integrin β1 of neonatal CMs: Neonatal CMs cultured on aligned collagen-coated coverslips were fixed at culture stages of 4, 18, 48, and 72 h. The fixed sample was first stained for integrin β1. It was blocked with 1% BSA, 4% donkey serum, 0.025% Triton X-100, and PBS for 30 minutes at RT. Next, it was incubated with the first antibody, mouse-anti-rat integrin β1 (1:50, Santa Cruz Biotechnology, US), overnight at 4 °C. It was then incubated with the second antibody, Alexa fluor© 488 conjugated donkey-anti-mouse IgG (1:200, Life Technologies, US), at RT for 1.5 h in the dark. Then, the sample was stained for laminin using the same procedure and final treatment as described above.

Imaging of immunofluorescence staining results

The immunofluorescence-staining results were imaged by fluorescence microscope (Zeiss Axiovert 200M) or confocal microscope (Zeiss 510LSM) with a 63x/1.4 oil/plan-

Apochromat lens. The interval between Z-stack images was 0.8 μm. To semiquantitatively analyze BM-laminin development, all samples were scanned using the same microscopic settings: Pinhole ϕ 4.84 airy units; optical slice less than 3.91 μm; amplifier gain 1.24; offset 0.972; and detector gain 1115. For double-stained samples, two parallel channels of green and red were applied with amplifier gain and offset settings that were selected to achieve optimal image quality.

Analysis of BM-laminin development of neonatal CMs cultured on aligned collagen

The cross-sectional area of each cell obtained from an optical microscope and the corresponding area of the deposited BM-laminin obtained from a confocal microscope were calculated by ImageJ (NIH), and the ratios of BM-laminin coverage of the neonatal CMs at different culture stages were evaluated based on the following equation:

$$\mathrm{BMlaminin\ \ Coverage\ \ Ratio} = (\mathrm{BMlaminin\ \ area}) / (\mathrm{cell\ \ crosssectional\ \ area})$$

The ratio was averaged among 6 cells. The morphologies of the BM-laminin network were categorized into three types: dot, line, and circle. The number of cells that belonged to each type at each culture stage was calculated based on at least 30 individual cells. At 4 h, the orientation of the BM-laminin deposit on single neonatal CMs (N = 20) cultured on aligned collagen was evaluated by measuring the angle θ formed between the major axis of the deposited laminin pattern obtained from a confocal microscope and the major axis of the cell image obtained from a phase microscope, as shown in Figure SI-1 A, B, and C. The angle θ was used to study the relationship of BM-laminin deposition and neonatal CM polarity.

Colocalization analysis

The colocalization analysis was conducted with Just Another Colocalization Plugin (JACoP ImageJ, National Institute of Health). Images of red and green channels were transformed into 8-bit format, and Pearson's coefficients (PCs) were calculated from two images with the JACoP plugin.

Statistical analysis

All data are presented as mean ± SD. Two groups of variables were compared using Student's t-test. A value of $P < 0.05$ was considered significant.

Results

Development of a BM-laminin network surrounding single neonatal CMs

Figure 1 shows images of single neonatal CMs during formation of a BM-laminin network. At 1 h, laminin was deposited in a dot-like shape at a single point on the edge of the neonatal CM. After 4 h, laminin was seen in additional places along the cell border. At 20, 24, and 48 h, the cell was elongated in a spindle shape along the direction of collagen I alignment (32). Laminin deposition was observed to occur near the spindle poles of neonatal CMs along the culture timeline shown in Figure 1. We studied the relative distribution of laminin deposits at the poles of the neonatal CMs: At 4 h, 20 polarized cells were

quantitatively examined by calculating the angle θ shown in Figure SI-1 A, B and C. In Figure SI-1 D, the range of θ is between 0 to 30^{o}, indicating the primary initial laminin deposition was along the direction of cell polarization. At 72 h, laminin formed a fine fishnet-like network. To better examine the BM-laminin network's detailed structure, the samples were imaged with a confocal microscope (Figure 2). From 24-72 h (Figure 2A first row), cross-sectional 3D images showed that the BM-laminin network enclosed the surface of plasma membrane of each neonatal CM in an identifiable pattern. For each neonatal CM, the images of the bottom layers (Figure 2A, second row) show that, from 1-48 h, the ratio of BM-laminin coverage to the total area increased (Figure 2B). At 24 h and thereafter, the amount of deposited laminin was significant when compared to the deposition that occurred at 1 h and 4 h. During the same time period, the nascent BM-laminin network began to form (Figure 2A, second row).

BM-laminin network formation underwent three distinct morphological changes from 24-72 h (Figure 2A). At 24 h, the network had the appearance of dispersed dots; at 48 h, the dots were connected, forming lines; at 72 h, the lines were joined and formed polygonal rings that resembled polygonal circles (Figure 2A, second row). Figure 2C shows the results of statistical analysis of the percentage of cells with each morphological shape at 24, 48, and 72 h.

The BM-laminin network started to exhibit striated patterns from 48-to-72 h as shown in Figure 3A, with striation perpendicular to the direction of cell elongation. A similar pattern was observed in freshly isolated, laminin-stained adult CMs (Figure 3B) and in the tissue-section image of a ventricle from a 4-month-old rat (Figure 3D). The distance between two adjacent striations, L, was measured for neonatal CMs at 48 and 72 h and for freshly isolated adult CMs. As demonstrated in Figure 3C, for neonatal CMs at 48 h, L_{48} = 1.89±0.08 μm, and at 72 h, L_{72} = 2.06±0.06 μm; for adult CMs L_{ACM} = 2.02±0.04 μm. This showed significant differences between L_{48} and both L_{72} and L_{ACM} and that L_{48} is less than L_{72} and L_{ACM}.

Neonatal CM sarcomerogenesis and BM-laminin development

Laminin and α-actinin of neonatal CMs cultured from 4-72 h were double-immunofluorescence-stained to explore the relationship between sarcomerogenesis and development of the BM-laminin network. At 4 h, α-actinin formed a nonstriated structure (Figure 4A); laminin deposits were seen near it (Figure 4C and D), with colocalization on the edge (Figure 4E). At 18 h, α-actinin had started to form a striated structure (Figure 4F), and laminin deposits had increased and were distributed around the α-actinin (Figure 4I and J). From 48-72 h, the striated sarcomeric structures (Figure 4K and P) were more pronounced; deposited laminin had begun to noticeably colocalize with α-actinin (Figure 4N and S). Notably, the 3D structure at 72 h (Figure 4U) demonstrates that each Z-line of the striated myofibril overlapped one line of the striated laminin network. Here, the PC value was used to analyze the spatial relationship between laminin and α-actinin at different stages in culture. From 4-72 h, the PC value increased (Figure 4V): a substantial increase in PC value was observed between 4 and 18 h; there was negligible increase between the time points 18, 48, and 72 h.

At 18 h, two types of α-actinin were seen: 1) immature dot-like (Figure 5A, solid-line box), seen in nascent or premature myofibrils or Z-bodies, and 2) incompletely mature stria-like (Figure 5A, dashed-line rectangle), which formed the Z-lines (14). The BM-laminin distributions had a corresponding appearance (Figure 5A): The dot-like α-actinin of Z-bodies had laminin deposits near each α-actinin dot; the stria-like α-actinin of incompletely mature Z-lines had laminin aligned along the striations. The colocalization analysis (Figure 5B) demonstrated that the PC value, which measures the extent of laminin-α-actinin colocalization, was higher near maturing Z-lines than the Z-bodies. The colocalization in the Z-bodies appears as sparse dots; in the incompletely mature Z-lines, colocalization appears as lines (Figure 5A).

Finally, integrin β1 and laminin were double-immunofluorescence stained to demonstrate the relationship between BM-laminin network development and integrin organization. At 4 h, integrin β1 expressed on the neonatal CMs was scattered randomly; it had barely colocalized with laminin as (Figure 6 A - E). At 18 h, the area of colocalization between laminin and integrin β1 had increased (Figure 6 F - J). At 48 and 72 h, more integrin β1 was expressed, and its colocalization with laminin had increased (Figure 6 MK - T)

Discussion

In the myocardium, each CM is enclosed by a 50-100 nm-thick BM that is directly in contact with the plasma membrane (11). However, how the BM network wraps each single neonatal CM when it matures into an adult CM remains unknown. In our study, freshly isolated neonatal CMs from 3-day-old neonatal rats were seeded on an aligned collagen-coated coverslip that allowed neonatal CMs to grow along the collagen I fibers into the initial spindle- or rod-like phenotype. The neonatal CMs then aggregated and assembled, forming a structure that resembled cardiac-muscle fibers (2). This facilitated exploring in vivo-relevant features of BM-network development around a single CM. In vivo, collagen I, the major component of ECM, assembles into aligned fibers and regulates growth and differentiation of CMs (4, 30). To make use of collagen I's in vivo conformation to create an adult CM-like phenotype in vitro, Simpson et al. developed the aligned collagen method (27) to culture in vivo-like neonatal CMs (6). In our study, an aligned collagen coating was applied to facilitate neonatal CM differentiation into an adult CM-like phenotype to study the in vivo-relevant process of BM development (6). We are the first to report BM-laminin development as a CM grows from the neonatal stage into an adult-like CM: We observed that the initial (e.g., at 4 h) distribution of laminin deposits on single neonatal CMs in culture was concentrated mainly at the polarized ends (Figure 1). Consequently, the initially deposited laminin formed an elongated pattern, the axis of which was within 30 degree of the major axis of the cell's orientation (Figure SI-1). Our data suggest that BM-laminin deposition on the ends of neonatal CMs may be related to cellular growth and differentiation from the neonatal to the adult stage.

The network composed of laminin and other BM components intensively interacts with the cell body, surrounding it during its growth and differentiation. From the neonatal to the adult-like form, scattered dots on the cell surface become short lines, which become polygonal rings (Figure 2A second row). In comparison to the laminin deposition at 1 h, the

three laminin shapes (e.g., dot, line, and ring) at 48 h were found in approximately equal percentages, and the amount of laminin deposition had increased significantly—approximately 4-fold— (Figure 2B). A network composed of mostly polygonal-ring-shaped laminin formed at 72 h around most of the neonatal CMs (Figure 2C); this polygonal-ring morphology is intrinsic to laminin monomer self-assembly and is also found on the surface of myoblamyotubes (5, 36, 35, 34).

In some areas on several neonatal CMs at this transition period (48-72 h), the BM-laminin lines started to parallel each other to form a striated morphology (Figure 3A). At 48 h and 72 h, these stria had a spatial interval, L, of 1.89±0.08 μm and 2.06±0.06 μm, respectively (Figure 3C). Both the freshly harvested adult CMs and those from the ventricular sections of 4-month-old rats had well-formed, striated laminin structures; the value of L was 2.02±0.03 μm. An L value in the range of 1.8-2.0 μm is equal to the length of the sarcomere (the distance between adjacent Z-lines in heart-muscle fibers), suggesting that laminin distribution correlates with the location of Z-lines (25). In addition, although variation in the L value at 48 h was larger than that at 72 h (each BM-laminin line did not precisely align with its corresponding Z-line), the average values of L measured at various culture stages and from isolated or ex vivo adult CMs showed no significant difference between the corresponding sarcomeric lengths: The distance between Z-lines on the neonatal CMs in culture on the aligned collagen at 48 h was 1.83 ± 0.14 μm and 1.97 ± 0.10 μm at 72 h, which matches reported results (10, 21, 31). This suggests that the striated structure of both the BM network and the cardiac tissue that we observed in this study and that others have reported in the literature are developmentally related to the development of the sarcomeric structure.

Numerous researchers have reported that components of the BM (e.g., laminin and collagen IV) connect with integrins, which have been proven to respond via tyrosine phosphorylation of intracellular proteins to the bidirectional signal molecules between the ECM and the sarcomere (24). During signaling from outside the cell to inside the cell, integrin can sense mechanical stress exerted through the ECM and transduce it to the cytoskeletal structure to influence cell shape, migration, differentiation, and growth. During signaling from inside the cell to outside the cell, the conformation of the integrin cytoplasmic domain tail changes to activate and enhance integrin-ECM binding. Final formation of the ECM network may be regulated accordingly (9). However, the detailed interactive relationship between BM-network development and sarcomerogenesis during cardiac-cell differentiation from the neonatal to the adult stage is still unknown. In the study reported here, at 1 h α-actinin, an important component of premature myofibrils (14), was expressed along the peripheral edge of a spreading neonatal CM. After 4 h, laminin deposition was found near the expressed α-actinin (Figure 4D and E). This suggests that premature myofibrils assembled before the deposition of laminin outside the plasma membrane. The double immunofluorescence staining shows that laminin and integrin β1 were expressed as dot-like shapes (Figure 6C and D) without obvious colocalization (Figure 6E), which suggests that the initial deposition of BM-laminin may not require the presence of β1 integrin (20). At 18 h, some α-actinin had started to demonstrate a striated structure on the edge of neonatal CMs (Figure 4I), indicating the beginning of Z-line formation (14). Laminin deposition appeared as scattered dots (Figure 5A) that encircled the Z-bodies (28) composed of nonstriated α-actinin (Figure

5A). At this time, laminin deposits were also seen near integrins, with colocalization on the interface (Figure 6I and J). With development of the cell, larger colocalized areas (higher PC value) of the BM-laminin network and the α-actinin pattern (Figure 4O and T) and of the BM-laminin network and integrins (Figure 6O and T) were observed near incompletely mature striated Z-lines, suggesting that laminin tended to be distributed near Z-lines and integrins (14). The increase in PC value from 4-72 h indicates an increase in the colocalized area of laminin and α-actinin (Figure 4T). The orthogonal view (Figure 4U) of the laminin and α-actinin structures demonstrates that at 72 h, full colocalization was attained. This was observed by another group using a transmission electron microscope, which showed dense BM-laminin expression aligned with the Z-lines (7, 37). The relationship between BM-network formation and sarcomerogenesis is illustrated in Schematic 1. The initial deposit of BM-laminin at 4 h shows a small area of colocalization of Z-bodies and integrins; Z-bodies assembled earlier than BM-laminin. Integrin was the bridge between Z-lines and the BM-laminin and was expressed even earlier than Z-bodies (28). At 18 h, the BM-laminin encircled the Z-bodies and colocalized with incompletely mature Z-lines and integrins on the interface. At 48 h, the BM-laminin reassembled and was deposited at positions near Z-lines and integrins. From approximately 72 h, these three structures were colocalized. The results suggest that spatial development of the BM-laminin network outside the plasma membrane is related to the sarcomerogenesis of CMs inside the plasma membrane via the bridge of integrin on the plasma membrane. Consequently, the final formation of the BM-laminin network from the neonatal to the adult stage is the result of interaction between the BM-laminin network and the sarcomeric structure mediated by integrin.

Conclusions

To summarize, the relative distributions in the development of BM-laminin, Z-line-α-actinin, and integrin β1 on a single neonatal CM cultured on an aligned collagen substrate were studied using confocal microscopy and colocalization analysis. The results were compared with adult ventricular-tissue sections and adult CMs. It was found that development of the BM-laminin network from the neonatal to the adult stage is closely related to sarcomeric formation via integrin-mediated interactions.

Supplementary Material

Refer to Web version on PubMed Central for supplementary material.

Acknowledgments

This work was partially supported by National Institutes of Health (P20RR021949, R01HL124782, and 5R01HL085847) and American Heart Association (14GRNT20520004). The authors would like to thank Dr. Terri Bruce in Clemson Light Imaging Facility for the help with confocal microscopy.

References

1. Abrahamson DR. Development of kidney glomerular endothelial cells and their role in basement membrane assembly. Organogenesis. 2009; 5(1):275–287. [PubMed: 19568349]
2. Baudino TA, Carver W, Giles W, Borg TK. Cardiac fibroblasts: friend or foe? Am J Physiol Heart Circ Physiol. 2006; 291(3):H1015–1026. [PubMed: 16617141]

3. Borg TK, Gay RE, Johnson LD. Changes in the distribution of fibronectin and collagen during development of the neonatal rat heart. Coll Relat Res. 1982; 2(3):211–218. [PubMed: 6759014]
4. Borg TK, Goldsmith EC, Price R, Carver W, Terracio L, Samarel AM. Specialization at the Z line of cardiac myocytes. Cardiovascular Research. 2000; 46(2):277–285. [PubMed: 10773232]
5. Colognato H, Winkelmann DA, Yurchenco PD. Laminin polymerization induces a receptor-cytoskeleton network. J Cell Biol. 1999; 145(3):619–631. [PubMed: 10225961]
6. Farhadian F, Contard F, Sabri A, Samuel JL, Rappaport L. Fibronectin and basement membrane in cardiovascular organogenesis and disease pathogenesis. Cardiovasc Res. 1996; 32(3):433–442. [PubMed: 8881506]
7. Frank JS, Brady AJ, Farnsworth S, Mottino G. Ultrastructure and function of isolated myocytes after calcium depletion and repletion. Am J Physiol. 1986; 250(2 Pt 2):H265–275. [PubMed: 3946627]
8. Hallmann R, Horn N, Selg M, Wendler O, Pausch F, Sorokin LM. Expression and function of laminins in the embryonic and mature vasculature. Physiol Rev. 2005; 85(3):979–1000. [PubMed: 15987800]
9. Israeli-Rosenberg S, Manso AM, Okada H, Ross RS. Integrins and integrin-associated proteins in the cardiac myocyte. Circ Res. 2014; 114(3):572–586. [PubMed: 24481847]
10. Kontrogianni-Konstantopoulos A, Catino DH, Strong JC, Bloch RJ. De novo myofibrillogenesis in C2C12 cells: evidence for the independent assembly of M bands and Z disks. Am J Physiol Cell Physiol. 2006; 290(2):C626–637. [PubMed: 16207790]
11. Langer GA, Frank JS. Lanthanum in heart cell culture. Effect on calcium exchange correlated with its localization. J Cell Biol. 1972; 54(3):441–455. [PubMed: 5044754]
12. Langer GA, Frank JS, Nudd LM, Seraydarian K. Sialic acid: effect of removal on calcium exchangeability of cultured heart cells. Science. 1976; 193(4257):1013–1015. [PubMed: 948758]
13. Leivo I, Vaheri A, Timpl R, Wartiovaara J. Appearance and distribution of collagens and laminin in the early mouse embryo. Dev Biol. 1980; 76(1):100–114. [PubMed: 6991310]
14. Liu H, Shao Y, Qin W, Runyan RB, Xu M, Ma Z, Borg TK, Markwald R, Gao BZ. Myosin filament assembly onto myofibrils in live neonatal cardiomyocytes observed by TPEF-SHG microscopy. Cardiovasc Res. 2012
15. Lundgren E, Gullberg D, Rubin K, Borg TK, Terracio MJ, Terracio L. In vitro studies on adult cardiac myocytes: attachment and biosynthesis of collagen type IV and laminin. J Cell Physiol. 1988; 136(1):43–53. [PubMed: 3294238]
16. Ma Z, Yang HX, Liu HH, Xu MF, Runyan RB, Eisenberg CA, Markwald RR, Borg TK, Gao BZ. Mesenchymal Stem Cell-Cardiomyocyte Interactions under Defined Contact Modes on Laser-Patterned Biochips. PLoS One. 2013; 8(2)
17. McGarvey ML, Baron-Van Evercooren A, Kleinman HK, Dubois-Dalcq M. Synthesis and effects of basement membrane components in cultured rat Schwann cells. Dev Biol. 1984; 105(1):18–28. [PubMed: 6381174]
18. Miner JH. Organogenesis of the kidney glomerulus: focus on the glomerular basement membrane. Organogenesis. 2011; 7(2):75–82. [PubMed: 21519194]
19. Miner JH. The glomerular basement membrane. Exp Cell Res. 2012; 318(9):973–978. [PubMed: 22410250]
20. Nitkin RM, Rothschild TC. Agrin-induced reorganization of extracellular matrix components on cultured myotubes: relationship to AChR aggregation. J Cell Biol. 1990; 111(3):1161–1170. [PubMed: 2167896]
21. Rodriguez AG, Han SJ, Regnier M, Sniadecki NJ. Substrate stiffness increases twitch power of neonatal cardiomyocytes in correlation with changes in myofibril structure and intracellular calcium. Biophys J. 2011; 101(10):2455–2464. [PubMed: 22098744]
22. Roediger M, Miosge N, Gersdorff N. Tissue distribution of the laminin beta1 and beta2 chain during embryonic and fetal human development. J Mol Histol. 2010; 41(2-3):177–184. [PubMed: 20552257]
23. Ross RS, Pham C, Shai SY, Goldhaber JI, Fenczik C, Glembotski CC, Ginsberg MH, Loftus JC. Beta1 integrins participate in the hypertrophic response of rat ventricular myocytes. Circ Res. 1998; 82(11):1160–1172. [PubMed: 9633916]

24. Ross RS, Borg TK. Integrins and the myocardium. Circ Res. 2001; 88(11):1112–1119. [PubMed: 11397776]
25. Samarel AM. Costameres, focal adhesions, and cardiomyocyte mechanotransduction. Am J Physiol-Heart C. 2005; 289(6):H2291–H2301.
26. Shiraishi I, Simpson DG, Carver W, Price R, Hirozane T, Terracio L, Borg TK. Vinculin is an essential component for normal myofibrillar arrangement in fetal mouse cardiac myocytes. J Mol Cell Cardiol. 1997; 29(8):2041–2052. [PubMed: 9281437]
27. Simpson DG, Terracio L, Terracio M, Price RL, Turner DC, Borg TK. Modulation of cardiac myocyte phenotype in vitro by the composition and orientation of the extracellular matrix. J Cell Physiol. 1994; 161(1):89–105. [PubMed: 7929612]
28. Sparrow JC, Schock F. The initial steps of myofibril assembly: integrins pave the way. Nat Rev Mol Cell Biol. 2009; 10(4):293–298. [PubMed: 19190670]
29. Thyberg J, Hultgardh-Nilsson A. Fibronectin and the basement membrane components laminin and collagen type IV influence the phenotypic properties of subcultured rat aortic smooth muscle cells differently. Cell Tissue Res. 1994; 276(2):263–271. [PubMed: 8020062]
30. Tuzlakoglu K, Santos MI, Neves N, Reis RL. Design of nano- and microfiber combined scaffolds by electrospinning of collagen onto starch-based fiber meshes: a man-made equivalent of natural extracellular matrix. Tissue Eng Part A. 2011; 17(3-4):463–473. [PubMed: 20825361]
31. Wang X, Liu X, Wang S, Luan K. Myofibrillogenesis regulator 1 induces hypertrophy by promoting sarcomere organization in neonatal rat cardiomyocytes. Hypertens Res. 2012; 35(6): 597–603. [PubMed: 22418241]
32. Yang H, Borg TK, Wang Z, Ma Z, Gao BZ. Role of the Basement Membrane in Regulation of Cardiac Electrical Properties. Ann Biomed Eng. 2014
33. Yonghong Shao HL, Tong Ye, Tom Borg, Junle Qu, Xiang Peng, Hanben Niu, Bruce Gao. 3D Myofibril Imaging in Live Cardiomyocytes via Hybrid SHG-TPEF Microscopy. Proc of SPIE. 2011; 7903(79030F):79030F-79031–79030F-79035.
34. Yurchenco PD, Cheng YS. Self-assembly and calcium-binding sites in laminin. A three-arm interaction model. J Biol Chem. 1993; 268(23):17286–17299. [PubMed: 8349613]
35. Yurchenco PD, Amenta PS, Patton BL. Basement membrane assembly, stability and activities observed through a developmental lens. Matrix Biology. 2004; 22(7):521–538. [PubMed: 14996432]
36. Yurchenco PD. Basement membranes: cell scaffoldings and signaling platforms. Cold Spring Harb Perspect Biol. 2011; 3(2)
37. Zellner JL, Spinale FG, Eble DM, Hewett KW, Crawford FA. Alterations in Myocyte Shape and Basement-Membrane Attachment with Tachycardia-Induced Heart-Failure. Circulation Research. 1991; 69(3):590–600. [PubMed: 1873861]

Abbreviations

BM	basement membrane
ECM	extracellular matrix
neonatal CMs	neonatal cardiomyocytes
CMs	cardiomyocytes
GBM	glomerular BM
SD	Sprague–Dawley
DPBS	phosphate buffered saline
KRB	Kreb's Ringer bicarbonate buffer
DMEM	Dulbecco's Modified Eagle's Medium

RT	room temperature
JACoP	Just Another Colocalization Plugin
PCs	Pearson's coefficients
EB	embryoid body

Highlights

- Development of the basement membrane network from neonatal stage to adulthood is closely related to sarcomeric formation
- Basement-membrane laminin, sarcomeric Z-line, and transmembrane integrin all developed coordinately across a striated stage
- The three striated structures had significant colocalizations evaluated using Pearson's Correlation Coefficients

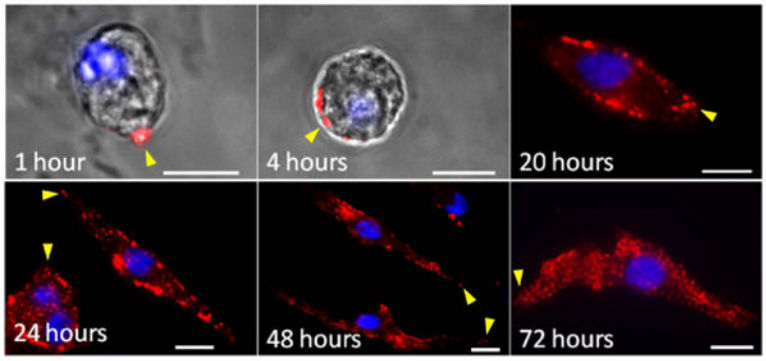

Figure 1.

Fluorescent images of BM-laminin structure at 1, 4, 20, 24, 48, and 72 h. Laminin in red, DAPI in blue. Arrowheads point to the polarized end of neonatal CMs. Scale bars: 10 μm.

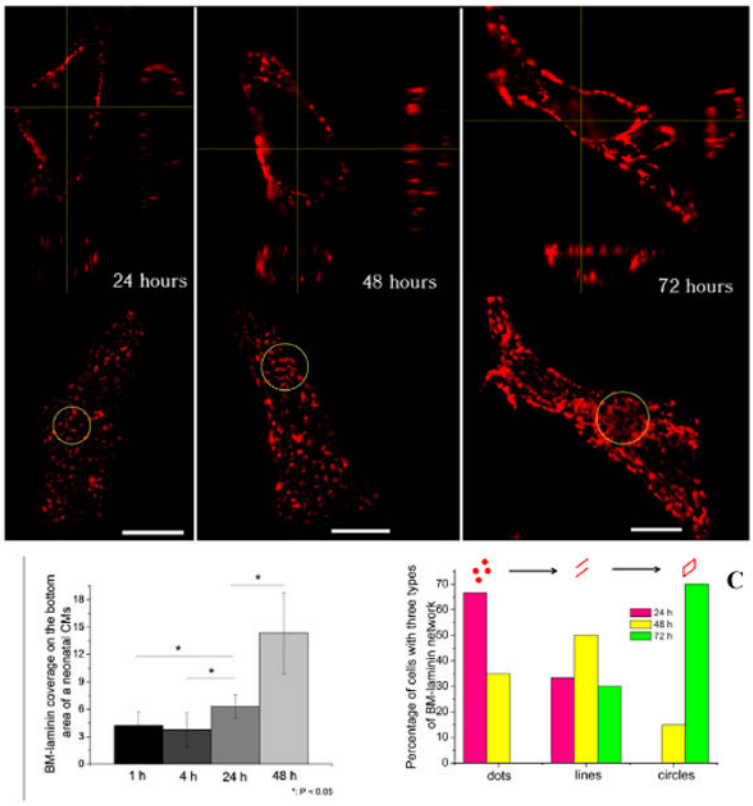

Figure 2.

(A) Orthogonal view of 3D structure of BM-laminin at 24, 48, and 72 h, corresponding BM-laminin network at each time point; circled areas indicate typical morphologies of BM-laminin network at each time point; scale bars: 10 μm; (B) Basement membrane coverage at 1, 4, 24, and 48 h based on the confocal and phase contrast images of 12 neonatal CMs at each time point, *: $P < 0.05$; (C) Percentage of cells with network of dot-, line-, and circle-shaped BM-laminin at 24, 48, and 72 h. Number of cells at each time point is 20.

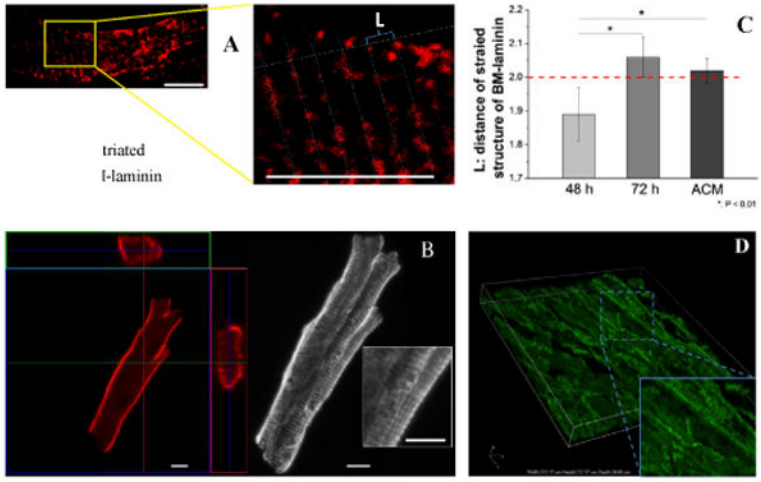

Figure 3.

(A) Striated structure of BM-laminin on a neonatal CM in culture on aligned collagen at 48 h. L indicates the distance between two adjacent striations, scale bar: 10 μm; (B) Orthogonal view of BM-laminin structure of a freshly isolated adult CM (ACM, left), z-plot image from 15 layers of Z-stack (right), enlarged striated structure (rectangular box), scale bar: 10 μm; (C) Average L values of neonatal CM cultured at 48 and 72 h and of an ACM; dashed red line represents the L value of a typical adult cardiac-muscle fiber, *: $P < 0.01$, scale bar: 10 μm; (D) 3D side view of laminin-stained adult cardiac-muscle-tissue section at a thickness of 30 μm with enlarged image at right bottom corner.

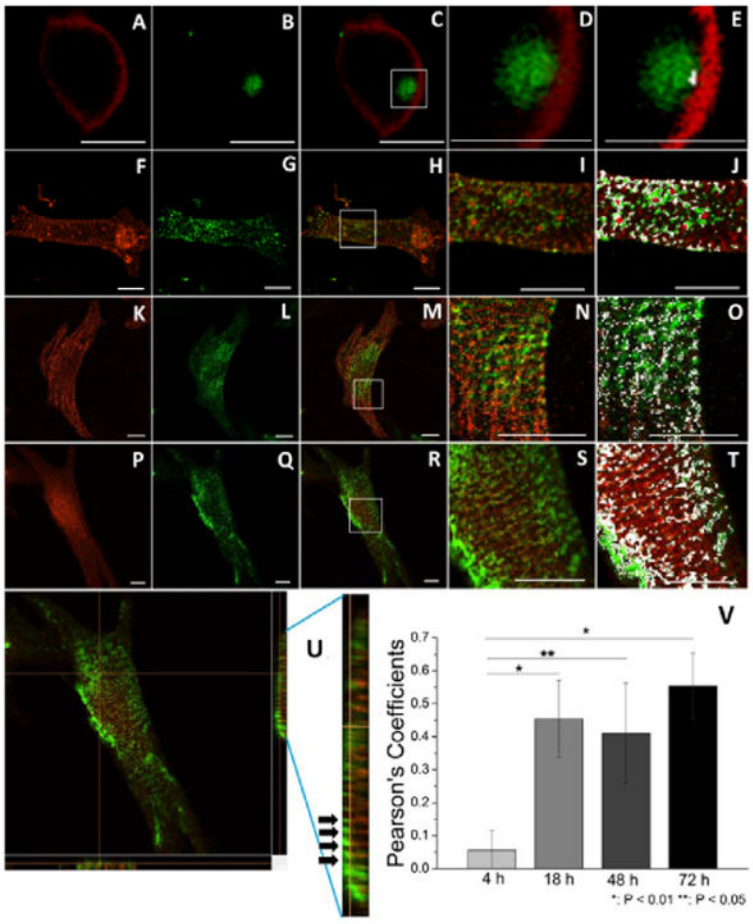

Figure 4.

Confocal images of laminin- and α-actinin-stained single neonatal CMs in culture on aligned collagen at 4, 18, 48, and 72 h. Red—images of α-actinin structure of neonatal CMs in culture for 4 (A), 18 (F), 48 (K), and 72 (P) h; Green—images of laminin structure of neonatal CMs in culture for 4 (B), 18 (G), 48 (L), and 72 (Q) h; merged images at 4 (C), 18 (H), 48 (M), and 72 (R) h; enlargements of the corresponding rectangular boxes at, 4 (D), 18 (I), 48 (N), and 72 (S) h; corresponding colocalized areas at 4 (E), 18 (J), 48 (O), and 72 (T) h, Scale bars: 10 μm. (U) Orthogonal view of 3D structure of laminin (green) and α-actinin (red) of neonatal CMs in culture on aligned collagen at 72 h; the rectangle on the right is the partially enlarged images of left-to-right side view; black arrows indicate the overlaid structure of laminin and α-actinin. (V) Pearson coefficients of laminin and α-actinin structures of neonatal CMs in culture on aligned collagen at 4, 18, 48, and 72 h, *: $P < 0.01$, **: $P < 0.05$, and $n = 3$ or 4. Scale bars: 10 μm.

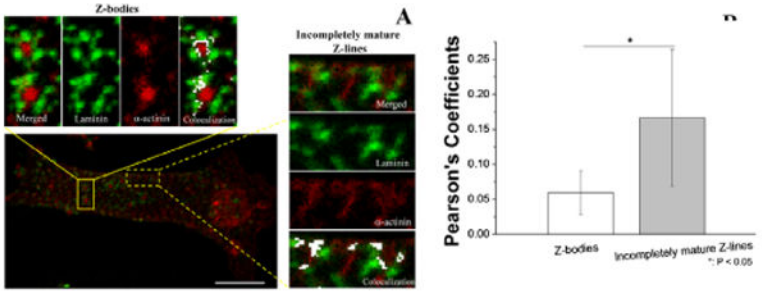

Figure 5.

(A) Confocal images and colocalization analysis of laminin and α-actinin of neonatal CMs in culture at 18 h. Solid-line rectangle: Z-bodies with dot-like α-actinin; dashed-line rectangle: incompletely mature Z-lines with striated α-actinin. Colocalized areas are in white. Scale bar: 10 μm. (B) Pearson's coefficients of corresponding images in A of Z-bodies and incompletely mature Z-lines. *: $P < 0.05$, $n = 5$.

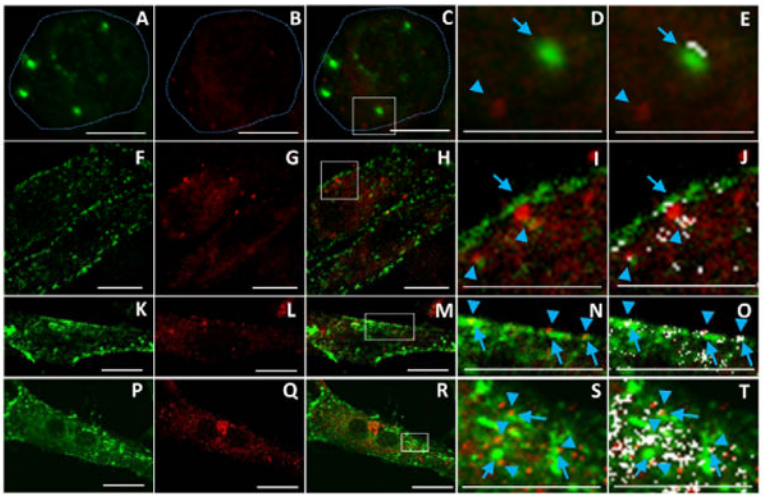

Figure 6.

Confocal images of laminin and integrin β1 staining of single neonatal CMs cultured on aligned collagen at 4, 18, 48, and 72 h. Images of laminin (green) in culture 4 (A), 18 (F), 48 (K), and 72 (P) h; images of integrin β1 (red) in culture 4 h (B), 18 (G), 48 (L), and 72 (Q) h; merged images at 4 (C), 18 (H), 48 (M), and 72 (R) h; D, I, N, and S are, respectively, enlarged images of the area in the rectangular box in C, H, M, and R; the same images, with the colocalized areas in white, are, respectively, presented at E, J, O, and T. Dashed lines in A, B, and C indicate outline of the neonatal CM. Arrows and arrowheads in D, E, I, J, N, O, S, and T indicate positions of laminin and integrin β1, respectively. Scale bars in A-C, F-H, K-M and P-R, 10 μm; in D and E, 8 μm; in I and J, 9 μm; in N and O, 12 μm; in S and T; 6 μm.

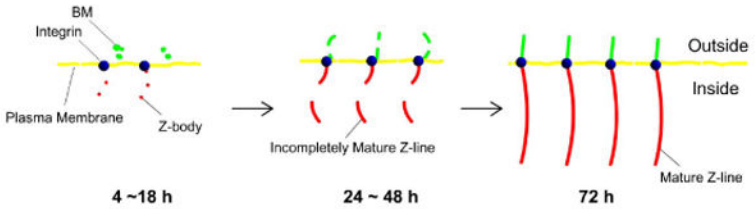

Schematic 1.

Illustration of the relationship between BM-laminin network development and sarcomerogenesis of a neonatal CM cultured on aligned collagen.